

# Unit Commitment with Joint Chance Constraints in Multi-area Power Systems with Wind Power Based on Partial Sample Average Approximation

Jinghua Li, Hongyu Zeng, and Yutian Xie

**Abstract**—Joint chance constraints (JCCs) can ensure the consistency and correlation of stochastic variables when participating in decision-making. Sample average approximation (SAA) is the most popular method for solving JCCs in unit commitment (UC) problems. However, the typical SAA requires large Monte Carlo (MC) samples to ensure the solution accuracy, which results in large-scale mixed-integer programming (MIP) problems. To address this problem, this paper presents the partial sample average approximation (PSAA) to deal with JCCs in UC problems in multi-area power systems with wind power. PSAA partitions the stochastic variables and historical dataset, and the historical dataset is then partitioned into non-sampled and sampled sets. When approximating the expectation of stochastic variables, PSAA replaces the big- $M$  formulation with the cumulative distribution function of the non-sampled set, thus preventing binary variables from being introduced. Finally, PSAA can transform the chance constraints to deterministic constraints with only continuous variables, avoiding the large-scale MIP problem caused by SAA. Simulation results demonstrate that PSAA has significant advantages in solution accuracy and efficiency compared with other existing methods including traditional SAA, SAA with improved big- $M$ , SAA with Latin hypercube sampling (LHS), and the multi-stage robust optimization methods.

**Index Terms**—Unit commitment, joint chance constraint, renewable energy, multi-area power system, wind power, sample average approximation, partial sample average approximation.

## NOMENCLATURE

### A. Indices and Sets

$A_k$	Set of areas connected with area $k$
$g$	Index of thermal power units
$G_k$	Set of thermal power units in area $k$
$K$	Set of areas
$k, l$	Indices of areas
$N$	Set of wind power samples

$n, s$	Indices of wind power samples
$t$	Index of scheduling hours
$T$	Set of scheduling time horizon

### B. Binary Variables

$d_i^{l,k}$	State of tie-line from area $l$ to area $k$ at hour $t$
$u_{g,t}^k$	State of unit $g$ in area $k$ at hour $t$
$z_t^n$	Binary variable of sample $n$ at hour $t$
$z_t^s$	Binary variable of sample $s$ at hour $t$

### C. Continuous Variables

$P_{g,t}^k$	Power of unit $g$ in area $k$ at hour $t$
$P_{W,t}^k$	Wind power of area $k$ at hour $t$
$P_{WH,t}^{k,m}$	Historical sample $m$ of $P_{W,t}^k$ in area $k$ at hour $t$
$\bar{P}_g^k, \underline{P}_g^k$	Upper and lower power bounds of unit $g$ in area $k$ at hour $t$
$R_{g,t}^{P,k}, R_{g,t}^{N,k}$	Positive and negative spinning reserves supplied by unit $g$ in area $k$ at hour $t$
$R_t^{P,k}, R_t^{N,k}$	Positive and negative spinning reserves of area $k$ at hour $t$
$y_t^n$	Lower bound of probability of sample $n$ at hour $t$
$y_t^s$	Lower bound of probability of sample $s$ at hour $t$
$z_{1,t}^n, z_{2,t}^n$	Continuous variables of sample $n$ at hour $t$
$z_{1,t}^s, z_{2,t}^s$	Continuous variables of sample $s$ at hour $t$

### D. Parameters

$\varepsilon$	Confidence level
$\eta$	Coefficient of spinning reserve requirement
$M_{k,t}^n$	A large enough constant of sample $n$ in area $k$ at hour $t$
$\bar{p}^{l,k}, \underline{p}^{l,k}$	Upper and lower power bounds of tie-line from area $l$ to $k$
$P_{WF,t}^k$	Forecasted wind power of area $k$ at hour $t$
$P_{W,t}^{k,n}$	Wind power of sample $n$ of area $k$ at hour $t$
$P_{L,t}^k$	Forecasted load of area $k$ at hour $t$
$T_{g,on}^k$	The minimum on time for unit $g$ in area $k$
$T_{g,off}^k$	The minimum off time for unit $g$ in area $k$

Manuscript received: December 30, 2023; revised: March 15, 2024; accepted: July 4, 2024. Date of CrossCheck: July 4, 2024. Date of online publication: July 29, 2024.

This work was supported by the National Natural Science Foundation of China (No. 51977042).

This article is distributed under the terms of the Creative Commons Attribution 4.0 International License (<http://creativecommons.org/licenses/by/4.0/>).

J. Li (corresponding author), H. Zeng, and Y. Xie are with the School of Electrical Engineering, Guangxi University, Nanning 530004, China (e-mail: lijinghua@gxu.edu.cn; zhy184267@163.com; xyt1239006190@163.com).

DOI: 10.35833/MPCE.2023.001038

## I. INTRODUCTION

WITH the development of power systems with renewable energy sources, the source-load probability bal-



ance has become the main form of power balance. Due to the increasing complexity and diversity of renewable energy sources, the coordination relationships among multiple areas have been strengthened. Thus, it has become a hot topic and challenging task to ensure the source-load probability balance among multiple areas.

Probability constraints, also known as chance constraints, are highly effective in handling the spinning reserve (SR) constraints in unit commitment (UC) problems [1]. Chance constraints belong to a single-objective function that utilizes probability metrics (confidence levels) to measure the risk posed to the scheduling decisions, ensuring that the resulting solution guarantees the fulfillment of constraints at the pre-set confidence level. Therefore, chance constraints cannot guarantee non-anticipative scheduling decisions.

Depending on the number of constraints that must be met simultaneously, chance constraints can be partitioned into joint chance constraints (JCCs) and individual chance constraints (ICCs). Compared with ICCs, JCCs can more accurately represent the interdependence between multiple wind farms, enabling the SR of multiple wind farms to simultaneously meet the power system requirements [2]. In general, JCCs are difficult to be solved directly because of the non-convex feasible set and complex multi-dimensional integration. Instead, JCCs are typically converted into deterministic constraints by other means, which can be easily solved using mature methods. Current conversion methods can be divided into two main types, i.e., analytical methods and simulation methods.

Analytical methods require the use of an assumed probability distribution function (PDF) of stochastic variables for conversion from stochastic to deterministic variables [3]. Some researchers have assumed that the outputs of renewable energy sources follow known PDFs such as the normal distribution [4], [5] and Weibull distribution [6]. These previously assumed PDFs are overly dependent on the subjective judgment of researchers, and errors between the assumed and actual PDFs result in inaccurate solutions.

Instead of assuming a PDF, some researchers have used the point estimate method [7], kernel density estimation [8], [9], and distributed robust chance-constrained method [10] to directly construct the PDF. However, these methods require the selection of suitable model parameters. Another analytical method known as  $p$ -efficient points [11], [12] uses an empirical distribution function (EDF) instead of constructing a PDF. In addition, [13] uses Boole's inequalities to partition JCCs into a series of ICCs. However, no suitable method exists for allocating the intersection probability [14].

Thus, most analytical methods involve the calculation of the PDFs of stochastic variables, which is a complex process for calculating multi-dimensional integrals. Alternatively, simulation methods do not rely on the PDFs of stochastic variables and are entirely data-driven, making the process of solving JCCs simpler and easier.

Classical simulation methods include Monte Carlo (MC)-based methods, which approximate the probability of satisfying chance constraints through stochastic sampling and com-

putations [15]. MC-based methods improve the approximation accuracy by using many MC samples, which results in increased computation time. To avoid this drawback, the importance sampling method [16] and ninth-order polynomial normal conversion technique [17] are combined with MC sampling to improve the performance.

Sample average approximation (SAA) uses the mean of MC samples to approximate the expectations of stochastic variables [18]-[20]. Notably, SAA employs the big- $M$  formulation during the solution process, which introduces many binary variables, eventually resulting in a large-scale mixed-integer programming (MIP) problem that severely restricts the computation efficiency [21], [22].

To avoid this drawback, the big- $M$  formulation is combined with a strong extended formulation in [23], [24] to improve the accuracy of approximation. An arbitrarily selected  $M$  value in SAA may result in a poor linear programming relaxation bound [25], which dynamically decreases the accuracy of the optimal solution. Reference [26] combines SAA with Latin hypercube sampling (LHS) to obtain a better result of approximation. In addition, some studies have proposed combining cutting [27] and decomposition [28] algorithms to accelerate the solution process for MIP problems.

The aforementioned studies focus on improving the accuracy of conversion and the efficiency of handling large-scale MC samples. However, they have not fundamentally solved the problem of introducing many binary variables into SAA methods. Thus, the problem of low computation efficiency remains unsolved [29].

To further improve the SAA methods, this paper proposes an improved simulation method called partial sample average approximation (PSAA). Recently, the PSAA is applied in [30] to a distributed power generation planning problem and achieves good results. Note that PSAA has yet to be applied to UC problems with JCCs and is therefore the main focus of this paper. The PSAA partitions the stochastic variables and historical datasets, obtains MC samples only from the sampled set, and ultimately obtains deterministic constraints containing only continuous variables. The contributions of this paper are summarized as follows.

1) This paper proposes the PSAA to replace the assumed cumulative distribution function (CDF) with the big- $M$  formulation introduced by SAA, thereby avoiding the introduction of binary variables.

2) This paper applies PSAA to solve the UC problems with JCCs in multi-area power system with wind power (MAS-WP). It provides the basis guidance of PSAA to partition stochastic variables and finally obtains a set of efficient methods to solve the UC problems.

The remainder of this paper is organized as follows. Section II describes the mathematical formulation of UC problems with JCCs in MAS-WP. The solution process and shortcomings of SAA are introduced in Section III. The solution process and advantages of the PSAA are analyzed in Section IV. Section V presents the solution steps based on PSAA. Case studies are presented in Section VI. Section VII concludes this paper.

## II. MATHEMATICAL FORMULATION

### A. Mathematical Model

The mathematical model consists of two parts: objective functions and constraints. The constraints include power balance, tie-line, and thermal power unit constraints. For brevity, this paper presents only a mathematical model of the SR constraints. The remaining objective functions and constraints can be found in [12].

We focus on investigating the SR constraints in the form of chance constraints in the aforementioned mathematical model. For a single thermal unit, the positive SR (PSR) and negative SR (NSR) constraints are formulated as:

$$0 \leq R_{g,t}^{P,k} \leq \min\left(\bar{p}_g^k - p_{g,t}^k, u_{g,t}^k p_g^{U,k}\right) \quad \forall g \in G_k, \forall t \in T, \forall k \in K \quad (1)$$

$$0 \leq R_{g,t}^{N,k} \leq \min\left(p_{g,t}^k - \underline{p}_g^k, u_{g,t}^k p_g^{D,k}\right) \quad \forall g \in G_k, \forall t \in T, \forall k \in K \quad (2)$$

For the entire MAS-WP, the PSR and NSR constraints for each area should satisfy:

$$R_t^{P,k} = \sum_{g \in G_k} \left(p_{g,t}^k + R_{g,t}^{P,k}\right) + P_{w,t}^k + \sum_{l \in A_k} d_t^{l,k} \bar{p}^{l,k} - P_{L,t}^k \geq \eta P_{L,t}^k \quad k=1, 2, \dots, K, \forall t \in T \quad (3)$$

$$R_t^{N,k} = P_{L,t}^k + \sum_{l \in A_k} d_t^{k,l} \bar{p}^{k,l} - \sum_{g \in G_k} \left(p_{g,t}^k - R_{g,t}^{N,k}\right) - P_{w,t}^k \geq \eta P_{L,t}^k \quad k=1, 2, \dots, K, \forall t \in T \quad (4)$$

Wind power is the most widely used renewable energy source in power systems. However, the inherent intermittency and uncertainty of wind power pose significant challenges to the scheduling and operation of power systems [5]. Therefore, wind power is selected as a stochastic variable in this paper. To ensure the safety and reliability of the power system during operation, the SR capacity is typically allocated as the maximum capacity of a single unit or a certain proportion (5%-10%) of the load. In this paper, as in [31],  $\eta$  is selected to be 10%.

### B. Normalization of JCCs

The SR is specifically used to deal with uncertainties in power system operations, and SR constraints are used to cope with stochastic variables [32]. To balance the safety and economy of power systems, this paper considers the SR constraints in the form of JCCs. The final PSR and NSR constraints are formulated as:

$$\Pr \left\{ \sum_{g \in G_k} \left(p_{g,t}^k + R_{g,t}^{P,k}\right) + P_{w,t}^k + \sum_{l \in A_k} d_t^{l,k} \bar{p}^{l,k} - P_{L,t}^k \geq \eta P_{L,t}^k, \quad k=1, 2, \dots, K \right\} \geq \varepsilon \quad \forall t \in T \quad (5)$$

$$\Pr \left\{ P_{L,t}^k + \sum_{l \in A_k} d_t^{k,l} \bar{p}^{k,l} - \sum_{g \in G_k} \left(p_{g,t}^k - R_{g,t}^{N,k}\right) - P_{w,t}^k \geq \eta P_{L,t}^k, \quad k=1, 2, \dots, K \right\} \geq \varepsilon \quad \forall t \in T \quad (6)$$

The part containing the wind power output  $P_{w,t}^k$  is moved from the left sides in (5) and (6) to the right sides. The re-

maining parts are then moved to the left side of the inequality. Then, they are replaced with  $X_t^k$  and  $Y_t^k$  from (7) and (8).

$$X_t^k = -(1+\eta)P_{L,t}^k + \sum_{l \in A_k} d_t^{l,k} \bar{p}^{l,k} + \sum_{g \in G_k} \left(p_{g,t}^k + R_{g,t}^{P,k}\right) \quad k=1, 2, \dots, K, \forall t \in T \quad (7)$$

$$Y_t^k = (1-\eta)P_{L,t}^k + \sum_{l \in A_k} d_t^{k,l} \bar{p}^{k,l} - \sum_{g \in G_k} \left(p_{g,t}^k - R_{g,t}^{N,k}\right) \quad k=1, 2, \dots, K, \forall t \in T \quad (8)$$

Thus, the final normalizations are obtained as:

$$\Pr \left\{ X_t^k \geq -P_{w,t}^k, k=1, 2, \dots, K \right\} \geq \varepsilon \quad \forall t \in T \quad (9)$$

$$\Pr \left\{ Y_t^k \geq P_{w,t}^k, k=1, 2, \dots, K \right\} \geq \varepsilon \quad \forall t \in T \quad (10)$$

### C. Analysis of Difficulties in Solving JCCs

The general expressions of (9) and (10) are formulated as (11), which contains the multi-dimensional stochastic variable  $\mathbf{z} = [z_1, z_2, \dots, z_k, \dots, z_K]^T$ , the decision variable  $\mathbf{x}$ , and the  $k^{\text{th}}$  internal constraint  $g_k(\mathbf{x})$ .

$$\Pr \left\{ g_k(\mathbf{x}) \geq z_k, k=1, 2, \dots, K \right\} \geq \varepsilon \quad (11)$$

In (11),  $K$  inequalities exist, and the number of inequalities is equal to the dimension of stochastic variables. When traditional simulation methods are used to solve JCCs, it is necessary to obtain MC samples for each dimension of the stochastic variables. When the dimension of the stochastic variables increases, the number of MC samples also increases exponentially, resulting in a significantly reduced computation efficiency.

## III. SAA

### A. Solution Process for SAA

Specifically, SAA introduces the linear programming of big- $M$  formulation, which discretizes chance constraints into multiple deterministic constraints. We then calculate the number of deterministic constraints that must be satisfied based on the given confidence level. Finally, the satisfaction of each deterministic constraint is evaluated using MC samples, and feasible solutions are iteratively computed.

The conversion of JCCs based on SAA involves the following three steps, where (9) is used as an example for explanation.

First, JCCs are represented as expectation:

$$\Pr \left\{ X_t^k \geq -P_{w,t}^k, k=1, 2, \dots, K \right\} = \mathbb{E} \left[ \mathbb{I} \left( X_t^k \geq -P_{w,t}^k, k=1, 2, \dots, K \right) \right] \quad (12)$$

where  $\mathbb{I}$  is the indicator function that takes the value of 1 if the condition is true and 0 otherwise; and  $\mathbb{E}$  is the expectation function.

Second, by replacing the stochastic variables with the MC samples obtained from the EDF, (12) becomes:

$$\mathbb{E} \left[ \mathbb{I} \left( X_t^k \geq -P_{w,t}^k, k=1, 2, \dots, K \right) \right] = \frac{1}{N} \sum_{n=1}^N \mathbb{I} \left( X_t^k \geq -P_{w,t}^k, k=1, 2, \dots, K \right) \quad (13)$$

where  $P_{w,t}^{k,n}$  ( $n=1,2,\dots,N$ ) is the MC sample obtained from the EDF of  $P_{w,t}^k$ .

Finally, based on the big- $M$  method [19], (13) serves as the subject for superposing a series of equivalent deterministic constraints as:

$$X_t^k + P_{w,t}^{k,n} + z_t^n M_{k,t}^n \geq 0 \quad k=1,2,\dots,K, n=1,2,\dots,N \quad (14)$$

$$\frac{1}{N} \sum_{n=1}^N z_t^n \leq 1 - \varepsilon \quad n=1,2,\dots,N \quad (15)$$

$$z_t^n \in \{0,1\} \quad n=1,2,\dots,N \quad (16)$$

where  $z_t^n$  ( $n=1,2,\dots,N$ ) is used to determine whether constraint (14) holds; and  $M_{k,t}^n$  is used to ensure that (14) remains true when  $z_t^n=1$ . The performance of SAA is significantly affected by the value of  $M_{k,t}^n$ , and the chosen method is detailed in [25].

Similarly, the chance constraint in (10) representing the NSR constraints can be converted as:

$$Y_t^k - P_{w,t}^{k,s} + z_t^s M_{k,t}^s \geq 0 \quad k=1,2,\dots,K, s=1,2,\dots,N \quad (17)$$

$$\frac{1}{N} \sum_{s=1}^N z_t^s \leq 1 - \varepsilon \quad s=1,2,\dots,N \quad (18)$$

$$z_t^s \in \{0,1\} \quad s=1,2,\dots,N \quad (19)$$

Finally, the intractable JCCs (9) and (10) are converted into the tractable deterministic constraints (14)-(16) and (17)-(19).

### B. Analysis of Shortcomings of SAA

After the JCCs are solved based on SAA, an MIP model containing binary variables  $z_t^n$  and  $z_t^s$  is obtained, which can be solved using MIP solvers. Note that the numbers of inequalities and binary variables introduced by SAA are related to the number of MC samples. This paper considers PSR and NSR constraints in the JCC form. If the dimension of the variables is  $K$  and  $N$  MC samples are obtained by a sampling historical dataset for each dimension, then  $2N$  binary variables and  $2NK$  inequalities are introduced.

## IV. PSAA

### A. Concept for Improving SAA

To overcome the shortcomings of SAA, this paper proposes a PSAA method to solve JCCs. Figure 1 shows the process for improving SAA.

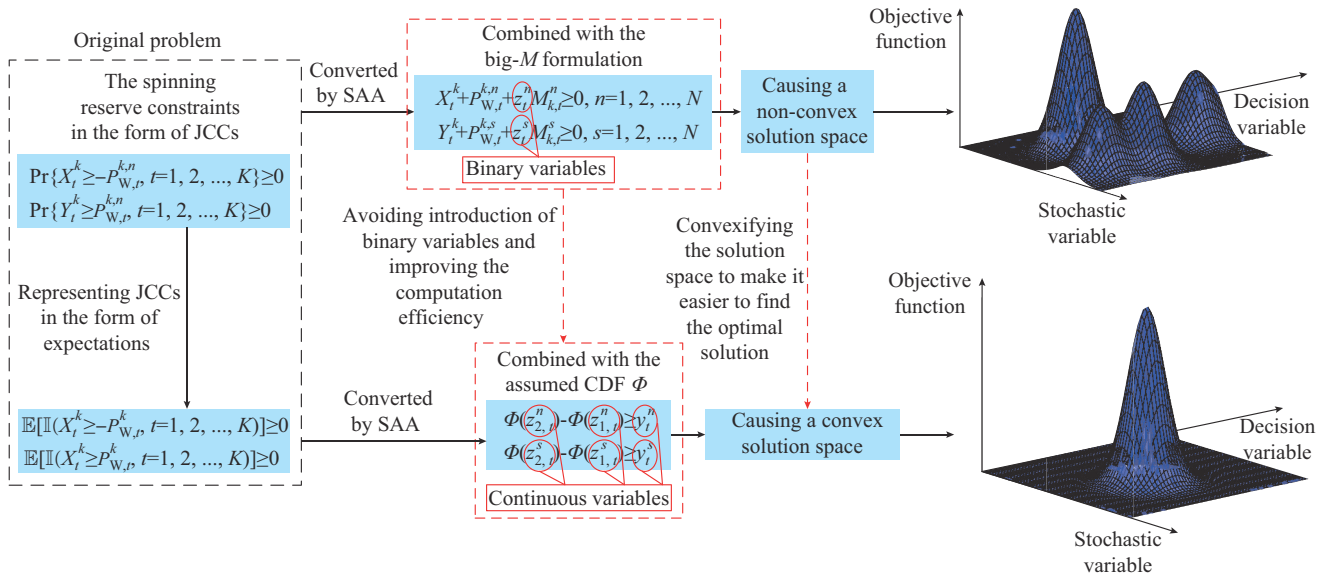


Fig. 1. Process for improving SAA.

### B. An Improved Method: PSAA

Two assumptions must be given before introducing the PSAA method.

Assumption 1: for the  $K$ -dimensional stochastic variable  $\xi = (\xi_1, \xi_2, \dots, \xi_K)$ , a one-dimensional variable  $\xi_1$  that is independent of the remaining  $(K-1)$ -dimensional variables exists.

Assumption 2: the independent one-dimensional stochastic variable follows a known continuous distribution such as the normal or uniform distribution.

Under these two assumptions, the process of PSAA is introduced in three steps.

#### 1) Partitioning Stochastic Variable and Historical Dataset

The stochastic variable  $P_{w,t}^k$  ( $k=1,2,\dots,K$ ) is partitioned into two parts:  $P_{w,t}^k$  ( $k=1$ ) and  $P_{w,t}^k$  ( $k=2,3,\dots,K$ ). For clari-

ty, we use the one-dimensional variable  $P_{w,t}^1$  to represent  $P_{w,t}^k$  ( $k=1$ ) and the  $(K-1)$ -dimensional variable  $\mathbf{P}_{w,t}^2$  to represent  $P_{w,t}^k$  ( $k=2,3,\dots,K$ ).

Similarly, the historical dataset corresponding to the stochastic variable must be partitioned. When the expectation of the stochastic variable is approximated using the mean of the MC samples, the error introduced is positively correlated with the variance of the historical dataset [29]. To reduce this error, we select the dimension with the largest variance as the non-sampled set and the others as the sampled set. Thus, the historical dataset is partitioned into a one-dimensional non-sampled set and a  $(K-1)$ -dimensional sampled set. Assume that  $P_{w,t}^1$  corresponds to the non-sampled set, whereas  $\mathbf{P}_{w,t}^2$  corresponds to the sampled set.

In Assumption 1,  $P_{w,t}^1$  represents the wind power output in

one area, and  $P_{W,t}^2$  represents the wind power output in the remaining  $K-1$  areas. In the MAS-WP considered in this paper, the correlation of wind farm output in a single area is relatively strong, whereas the correlation of wind farm output between areas is weak. Therefore, in the approximation process, the correlation is ignored. In related studies such as [33], [34], the correlation of wind farm output between areas is not considered. Therefore, based on Assumption 1, we consider  $P_{W,t}^1$ ,  $P_{W,t}^2$  and their expectations to be independent.

Still, we take (9) as an example, which can be reformulated as:

$$\Pr\{X_t^k \geq -P_{W,t}^k, k=1, 2, \dots, K\} = \mathbb{E}\left[\mathbb{I}\left(X_t^1 \geq -P_{W,t}^1, X_t^2 \geq -P_{W,t}^2\right)\right] \quad (20)$$

where  $X_t^2$  is the  $(K-1)$ -dimensional variable to represent  $X_t^k$  ( $k=2, 3, \dots, K$ ).

Lemma 1: let  $X$  and  $Y$  be independent stochastic variables that can be integrated, and  $g(X, Y)$  be a real-value function. If the expectation of  $g(X, Y)$  exists, we have:

$$\mathbb{E}[g(X, Y)] = \mathbb{E}_X[\mathbb{E}_Y[g(X, Y)]] = \mathbb{E}_Y[\mathbb{E}_X[g(X, Y)]] \quad (21)$$

According to Lemma 1, (20) can be formulated as:

$$\mathbb{E}_{P_{W,t}^1}\left[\mathbb{E}_{P_{W,t}^2}\left[\mathbb{I}\left(X_t^1 \geq -P_{W,t}^1, X_t^2 \geq -P_{W,t}^2\right)\right]\right] \geq \varepsilon \quad (22)$$

## 2) Approximating Expectation of Stochastic Variables

Similar to SAA, PSAA approximates the expectation of stochastic variables using the mean of the MC samples. The difference derives from the fact that PSAA only approximates the expectation of  $(K-1)$ -dimensional variables and not that of  $K$ -dimensional variables. Then, (22) can be formulated as:

$$\begin{aligned} \frac{1}{N} \sum_{n=1}^N \mathbb{E}_{P_{W,t}^1}\left[\mathbb{I}\left(X_t^1 \geq -P_{W,t}^1, X_t^2 \geq -P_{W,t}^{2,n}\right)\right] = \\ \frac{1}{N} \sum_{n=1}^N P\{X_t^1 \geq -P_{W,t}^1, X_t^2 \geq -P_{W,t}^{2,n}\} \geq \varepsilon \end{aligned} \quad (23)$$

where  $P_{W,t}^{2,n}$  ( $n=1, 2, \dots, N$ ) is the MC sample of  $P_{W,t}^2$ .

A normal distribution is commonly selected as the known distribution for wind power. Therefore, based on Assumption 2, this paper selects a normal distribution as the known distribution for  $P_{W,t}^1$  that corresponds to the non-sampled set. Therefore,  $\Phi(\cdot)$  represents the CDF of the normal distribution.

With the auxiliary continuous variable  $y_t^n$  ( $n=1, 2, \dots, N$ ) used to represent the confidence level, (24)-(26) are obtained.

$$\Pr\{X_t^1 \geq -P_{W,t}^1, X_t^2 \geq -P_{W,t}^{2,n}\} \geq y_t^n \quad n=1, 2, \dots, N \quad (24)$$

$$\frac{1}{N} \sum_{n=1}^N y_t^n \geq \varepsilon \quad (25)$$

$$y_t^n \geq 0 \quad n=1, 2, \dots, N \quad (26)$$

where  $y_t^n$  is the lower bound of the probability of the inequality  $X_t^1 \geq -P_{W,t}^1$  with  $X_t^2 \geq -P_{W,t}^{2,n}$  being satisfied.

## 3) Converting Chance Constraints into Deterministic Constraints

In (24), the conditions for inequalities  $X_t^1 \geq -P_{W,t}^1$  and  $X_t^2 \geq -P_{W,t}^{2,n}$  to hold are independent. We can then reformulate (24) as:

$$\Pr\{X_t^1 + X_t^k + P_{W,t}^{k,n} \geq -P_{W,t}^1\} \geq y_t^n \quad k=2, 3, \dots, K, n=1, 2, \dots, N \quad (27)$$

As  $P_{W,t}^1$  follows the distribution of  $\Phi(\cdot)$ , two continuous auxiliary variables  $z_{1,t}^n$  and  $z_{2,t}^n$  are introduced, which lie in the distribution of  $\Phi(\cdot)$  and satisfy  $z_{2,t}^n \geq P_{W,t}^1 \geq z_{1,t}^n$ . Thus, we have:

$$\Pr\{z_{2,t}^n \geq P_{W,t}^1 \geq z_{1,t}^n\} = \Phi(z_{2,t}^n) - \Phi(z_{1,t}^n) \quad (28)$$

Finally, we can obtain the deterministic constraints via (29)-(34).

$$X_t^1 + X_t^k + P_{W,t}^{k,n} \geq -z_{1,t}^n \quad k=2, 3, \dots, K, n=1, 2, \dots, N \quad (29)$$

$$X_t^1 + X_t^k + P_{W,t}^{k,n} \geq -z_{2,t}^n \quad k=2, 3, \dots, K, n=1, 2, \dots, N \quad (30)$$

$$\Phi(z_{2,t}^n) - \Phi(z_{1,t}^n) \geq y_t^n \quad n=1, 2, \dots, N \quad (31)$$

$$-\infty \leq z_{1,t}^n \leq z_{2,t}^n \leq +\infty \quad n=1, 2, \dots, N \quad (32)$$

$$\frac{1}{N} \sum_{n=1}^N y_t^n \geq \varepsilon \quad (33)$$

$$y_t^n \geq 0 \quad n=1, 2, \dots, N \quad (34)$$

Similarly, (10) can be converted to:

$$Y_t^1 + Y_t^k - P_{W,t}^{k,s} \geq z_{1,t}^s \quad k=2, 3, \dots, K, s=1, 2, \dots, N \quad (35)$$

$$Y_t^1 + Y_t^k - P_{W,t}^{k,s} \geq z_{2,t}^s \quad k=2, 3, \dots, K, s=1, 2, \dots, N \quad (36)$$

$$\Phi(z_{2,t}^s) - \Phi(z_{1,t}^s) \geq y_t^s \quad s=1, 2, \dots, N \quad (37)$$

$$-\infty \leq z_{1,t}^s \leq z_{2,t}^s \leq +\infty \quad s=1, 2, \dots, N \quad (38)$$

$$\frac{1}{N} \sum_{s=1}^N y_t^s \geq \varepsilon \quad (39)$$

$$y_t^s \geq 0 \quad s=1, 2, \dots, N \quad (40)$$

As (29)-(34) and (35)-(40) show, no binary variables exist. However, they have the same convergence as the SAA-based formulas of (14)-(16) and (17)-(19). In particular, when  $N$  increases, the obtained solution tends to approach the optimal solution.

For further details on the theoretical derivation and mathematical proof of the PSAA method, please refer to [35]. Supplementary Material A provides a detailed explanation of the concavity or convexity of constraints (31) and (37).

## C. Analysis of Advantages of PSAA

Next, the conversion results of (19) is examined. Figure 2 shows the solution processes of PSAA and SAA. Compared with SAA, PSAA has the following advantages.

### 1) Reducing Sample Scale

SAA samples are based on all historical datasets of stochastic variables, whereas PSAA first partitions the historical dataset into the non-sampled and sampled sets, which reduces the sample scale. In addition, as the error is an increasing function of the variance, to reduce this error, PSAA selects the one-dimensional historical dataset with the maximum variance as the non-sampled set and the remaining historical data as the sampled set.

### 2) Avoiding Introduction of Binary Variables

Comparing the SAA-based formulas of (14)-(16) with the PSAA-based formulas of (29)-(34), it can be seen that both

methods introduce auxiliary variables. However, SAA introduces  $N$  binary variables  $z_t^n$ , whereas PSAA introduces  $3N$  continuous variables  $z_{1,t}^n, z_{2,t}^n$  and  $y_t^n$ . Although the number of

introduced variables increases, it avoids many binary variables, which greatly improves the computation efficiency.

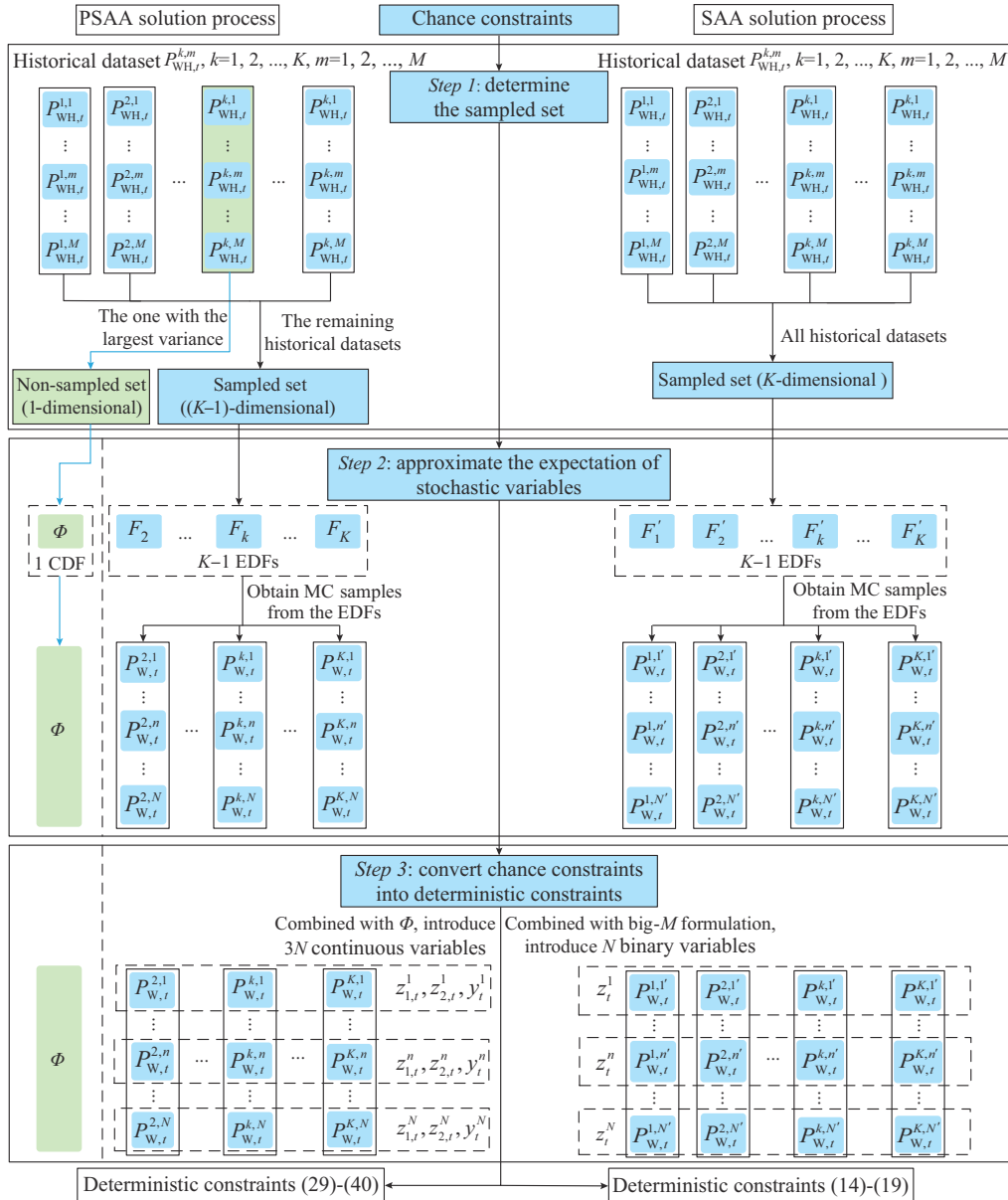


Fig. 2. Solution processes of PSAA and SAA.

## V. SOLUTION STEPS BASED ON PSAA

Figure 3 shows the solution steps based on PSAA, which are detailed as follows.

*Step 1:* establish a mathematical model that incorporates the PSR and NSR constraints in the UC problem using JCCs.

*Step 2:* standardize JCCs (5) and (6), and convert them into  $\Pr\{X_t^k \geq -P_{W,t}^k, k=1, 2, \dots, K\} \geq \varepsilon$  and  $\Pr\{Y_t^k \geq P_{W,t}^k, k=1, 2, \dots, K\} \geq \varepsilon$ , which facilitates subsequent mathematical derivation and exposition.

*Step 3:* partition the stochastic variable and historical dataset based on Section IV-B-1). The historical dataset  $P_{WH,t}^{k,m}$  ( $k=$

$1, 2, \dots, K, m=1, 2, \dots, M$ ) is partitioned into the non-sampled set  $P_{W,t}^1$  and the sampled set  $P_{W,t}^2$ .

*Step 4:* approximate the expectation of stochastic variables based on Section IV-B-2). Obtain MC samples  $P_{W,t}^{2,n}$  ( $n=1, 2, \dots, N$ ) from the EDF of the sampled set  $P_{W,t}^2$ , and use the normal distribution to replace the CDF of the non-sampled set  $P_{W,t}^1$ , thereby obtaining (24)-(26).

*Step 5:* convert JCCs into deterministic constraints based on Section IV-B-3). Obtain the MC samples from the sampled set and assume the CDF of the non-sampled set. Then, the MC samples and the assumed CDF are combined to mathematically derive the PSR deterministic constraints (29)-

(34) and NSR deterministic constraints (35)-(40).

*Step 6*: solve the UC model using the deterministic constraints of the existing solvers to obtain the scheduling information.

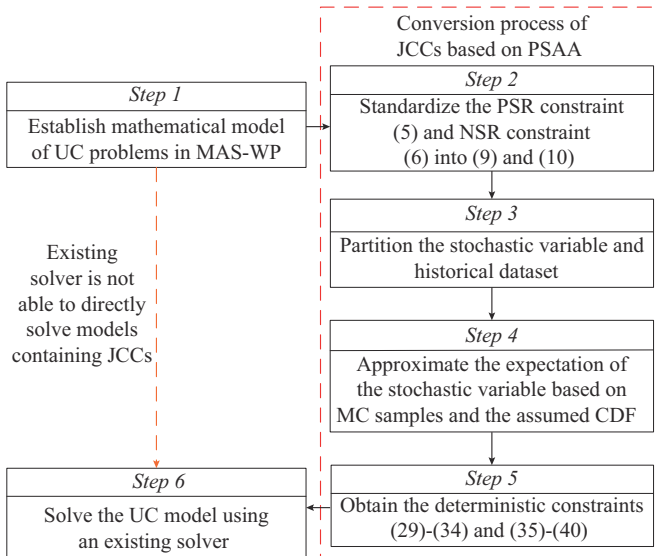


Fig. 3. Solution steps based on PSAA.

## VI. CASE STUDIES

### A. Case Descriptions

Two cases are considered in this paper. Case I represents a three-area system with 33 thermal units based on the IEEE 39-bus system. Area 1 consists of 10 thermal units and one wind farm with a capacity of 850 MW. Area 2 consists of 13 thermal units and one wind farm with a capacity of 1050 MW. Area 3 consists of 13 thermal units and one wind farm with a capacity of 1350 MW.

Case II represents a three-area system with 120 thermal units based on the IEEE 118-bus system. Area 1 consists of 33 thermal units and one wind farm with a capacity of 1600 MW. Area 2 consists of 33 thermal units and one wind farm with a capacity of 2500 MW. Area 3 consists of 54 thermal units and one wind farm with a capacity of 2800 MW.

In both cases, the scheduling horizon is 24 hours with a scheduling interval of one hour. Each scheduling interval has 730 historical samples of wind power, resulting in 17520 historical samples throughout the entire scheduling horizon. The historical samples are sourced from [36]. The other parameter settings in the simulation are as follows. The confidence level is set as  $\varepsilon=95\%$ , and the SR coefficient is set as  $\eta=10\%$ . JCCs are used to establish the SR constraints. Table I lists the simulation schemes.

In Case I, S1 and S2 apply SAA [19] and PSAA with 200 MC samples, respectively, whereas S3 and S4 have 400 MC samples. The purpose of the simulation is to compare not only the performances of the PSAA and SAA solutions but also the effects of the number of MC samples on the performances.

In Case II, S5-S8 have 400 MC samples, and the performances of SAA, SAA with the improved big- $M$  method (denoted as big- $M$ -SAA) [24], SAA with LHS (denoted as LHS-

SAA) [26], PSAA, and the multi-stage robust optimization (MSRO) method [37] are compared.

TABLE I  
SIMULATION SCHEMES

Case	Scheme	Method	Number of MC samples
I	S1	SAA	200
	S2	PSAA	200
	S3	SAA	400
	S4	PSAA	400
II	S5	SAA	400
	S6	Big- $M$ -SAA	400
	S7	LHS-SAA	400
	S8	PSAA	400
	S9	MSRO	

This paper focuses on solving the SR constraints in JCC form. Therefore, the comparison between the methods includes system operating cost, computation time, and SR.

### B. Simulation Results of Case I

#### 1) Verification of Feasibility of PSAA

Figure 4 shows the changes in the computation time and confidence levels of SAA and PSAA with an increase in sample size.

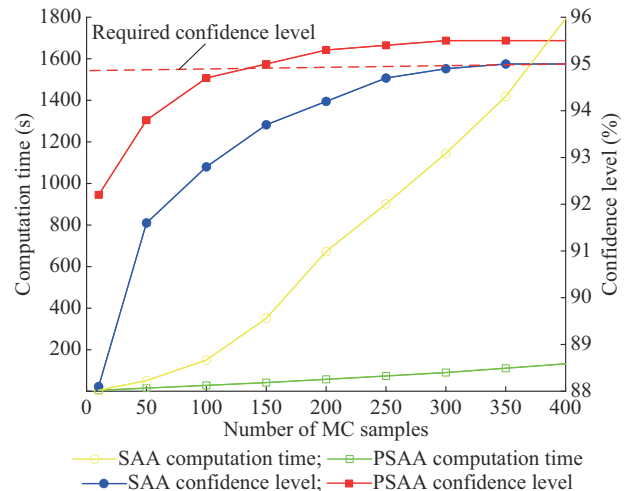


Fig. 4. Computation time and confidence levels of SAA and PSAA.

Figure 4 shows that the computation time for SAA and PSAA increases with the number of MC samples. When the sample size increases to 400, the computation time of SAA increases to approximately 1800 s, whereas that of PSAA increases only to approximately 200 s.

Both SAA and PSAA are unable to satisfy the system requirements when the number is less than 100. When the number increases to approximately 150, the confidence level of PSAA satisfies the system requirements. SAA requires 350 samples to satisfy a confidence level of 95%.

Table II shows that as the confidence level increases, both methods require an increase in the number of MC samples, with SAA requiring more samples than PSAA. In addition,

in the same range of increased confidence levels, SAA requires even more samples than PSAA. However, as the confidence level increases, the number of MC samples required by both methods does not increase continuously. The confidence level obtained by SAA is in the range of approximately 95.1%-95.5%, whereas for PSAA, it is in the range of approximately 95.6%-96.0%.

TABLE II  
CONFIDENCE LEVELS OF SAA AND PSAA

Set	Confidence level range (%)	Number of samples required for SAA	Number of samples required for PSAA
1	[92.0, 92.5)	70	10
2	[92.5, 93.0)	100	25
3	[93.0, 93.5)	120	40
4	[93.5, 94.0)	150	50
5	[94.0, 94.5)	180	70
6	[94.5, 95.0)	250	100
7	[95.0, 95.5)	380	150
8	[95.5, 96.0)		360

Figure 4 and Table II show that, as the sample size increases, the slopes of the two curves representing computation time remain relatively constant, whereas those of the two curves representing confidence level gradually decrease. When the sample size exceeds 200, the slope of the red curve decreases to 0, indicating that PSAA is less sensitive to the sample at this point. If the sample size is increased on this basis, the computation time will increase with little effect on the confidence level. However, the slope of the blue curve decreases to 0 only when the sample size exceeds 300, indicating that SAA requires a larger sample size. The sensitivity to the sample decreases with a sufficiently large sample size.

The previous comparative analysis shows that the performance of PSAA is less affected by the number of MC samples and can meet the system requirements using fewer samples. Moreover, PSAA has a stronger ability to deal with large-scale samples and has a higher computation efficiency.

2) Comparison of Results of S1 and S2

Figure 5 shows the PSR and NSR ratios of S1 and S2. The PSR and NSR ratios of both schemes satisfy the system requirements in Areas 1 and 2. In Area 3, the PSR and NSR ratios of S2 meet the system requirements. However, at 11:00 and 12:00, the NSR ratio of S1 is less than 10%, which does not meet the system requirements.

In addition, the fitness of SR allocation is verified in two respects: wind curtailment ratio and load loss ratio. Theoretically, the wind curtailment and load loss ratios should not exceed the risk level (5%).

Figure 6 shows the wind curtailment and load loss ratios of S1 and S2. In all three areas, the load loss ratio of both schemes is zero, which indicates that the PSR capacity of the system is sufficient. However, for the wind curtailment ratio, a significant difference is observed between S1 and S2. In Area 3, the results based on S2 exceed the boundary line at 10:00 and 12:00.

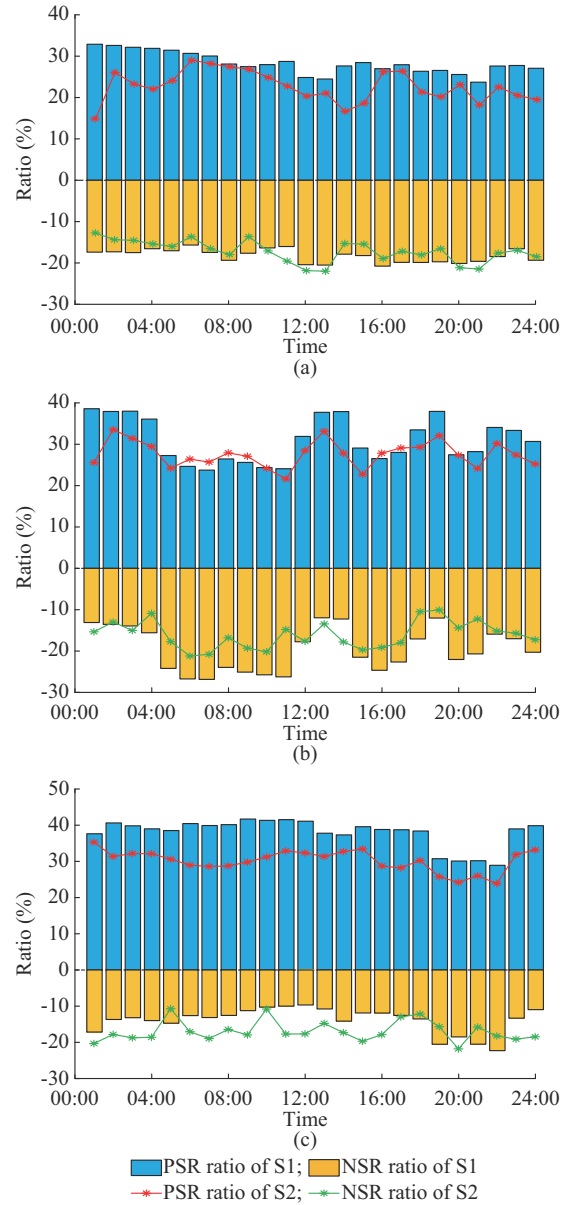


Fig. 5. PSR and NSR ratios of S1 and S2. (a) Area 1. (b) Area 2. (c) Area 3.

The aforementioned results indicate that when the sample size is 200, the scheduling results based on SAA cannot fully meet the system requirements. There are instances in certain scheduling intervals when the NSR ratio is too low and the wind curtailment ratio is too high. However, this problem does not exist in the scheduling results based on PSAA.

3) Comparison of Results of S3 and S4

Figure 7 shows the PSR and NSR ratios for S3 and S4. The PSR and NSR ratios at all scheduling time satisfy the system requirements.

Figure 8 shows the wind curtailment and load loss ratios of S3 and S4. The load loss ratios of S3 and S4 are zero in all three areas, indicating that the PSR ratios of the two schemes are sufficient. The load loss ratios of both schemes are no larger than 5% in the three areas, indicating that the NSR ratios in these three areas are sufficient.

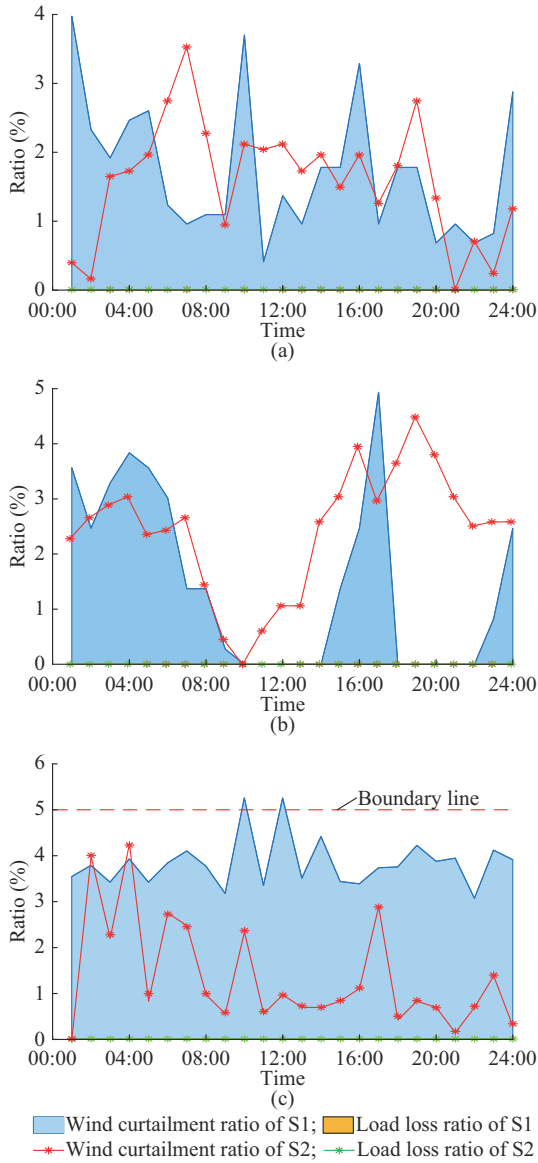


Fig. 6. Wind curtailment and load loss ratios of S1 and S2. (a) Area 1. (b) Area 2. (c) Area 3.

The results for S1-S4 show that there is little variation in the PSAA results when the sample size increases from 200 to 400. However, a significant change can be observed in the SAA results. After the sample size increases to 400, the SAA results for SR and wind curtailment ratios meet the system requirements. The aforementioned results again illustrate that, in contrast to PSAA, SAA is highly dependent on the sample size.

C. Simulation Results of Case II

Figure 9 shows the PSR and NSR ratios of S5-S9, which shows that the PSR and NSR ratios are higher than 10% during all scheduling time. In Area 1, the PSR ratio of S8 is higher than those of S5-S7 and S9, and the NSR ratio of S8 is lower than those of S5-S7. In Area 2, the PSR and NSR ratios of S9 are the highest, and the results of S5-S8 are basically the same. In Area 3, the PSR ratios of S5-S8 are basically the same. S9 has the lowest PSR ratio, and the NSR ratio of S8 is higher than those of S5-S7 and S9.

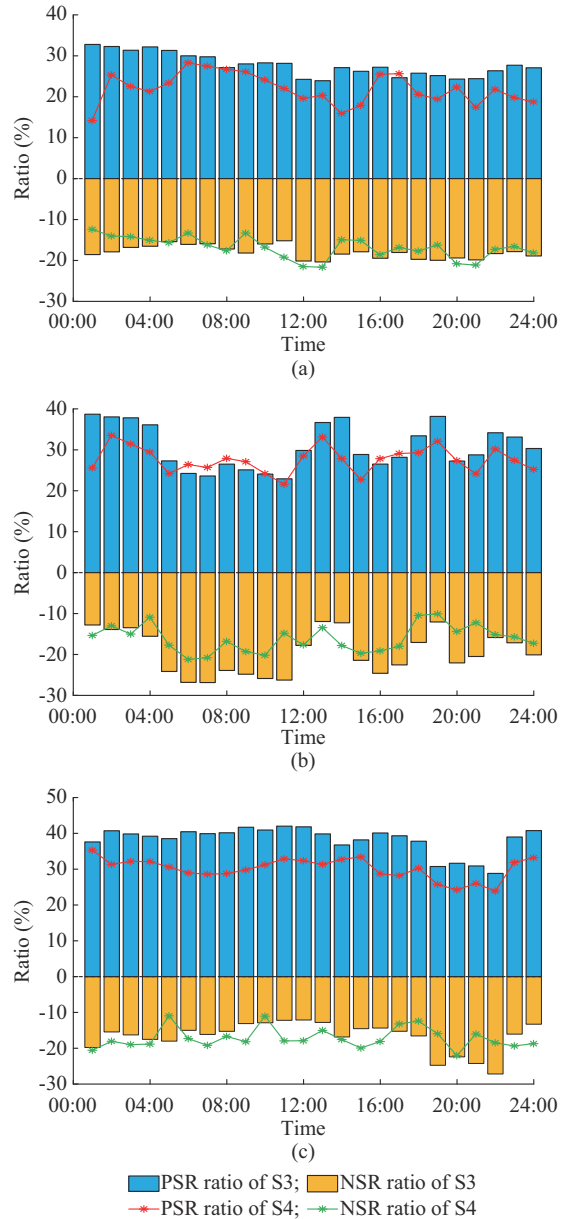


Fig. 7. PSR and NSR ratios of S3 and S4. (a) Area 1. (b) Area 2. (c) Area 3.

Figure 10 shows the wind curtailment and load loss ratios of S5-S9. In all three areas, the load loss ratios of S5-S9 are zero, and the wind curtailment ratios of S5-S7 are lower than those of S8 and S9. The comparative results show that among the four types of chance constraint-based methods, compared with SAA, big-M-SAA, and LHS-SAA, the solution results of the PSAA are the most accurate and least conservative. In addition, the PSAA is roughly equivalent to that of the MSRO.

D. Operating Cost and Computation Time

For Case I, when the MC sample size is 200, the operating cost of S1 is slightly less than that of S2. However, S2 has a much shorter computation time. When the sample size increases to 400, the computation time of S3 and S4 also increases.

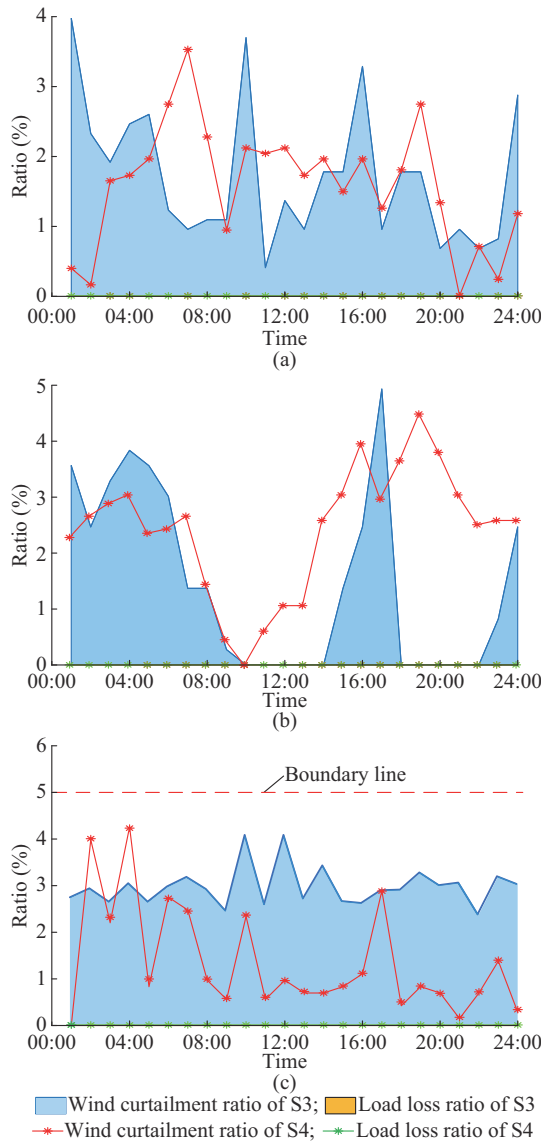


Fig. 8. Wind curtailment and load loss ratios of S3 and S4. (a) Area 1. (b) Area 2. (c) Area 3.

However, S4 still has a significant advantage. The operating cost of S3 increases compared with that of S1, because when the sample size is small, due to insufficient NSR, the solution of S1 does not meet the system requirements. Compared with that of S2, the variation of S4 is minimal, indicating that PSAA obtains a result that satisfies the system requirements, even with a small sample size.

For Case II, the operating costs of S5-S7 are basically the same, where S8 has a slightly higher operating cost, and S9 has the lowest operating cost. The computation efficiency of S9 is higher than those of S5-S7, but a time of more than 1000 s is still required. The solution speed of S8 is much faster than those of S5-S7 and S9, which only takes 204.65 s. For S5-S7, big-*M*-SAA has a higher solution efficiency. The comparison results indicate that the big-*M* method can simplify the computation complexity. However, the effects are not significant. The LHS-SAA mostly improves the sampling accuracy and has less effects on the computation efficiency.

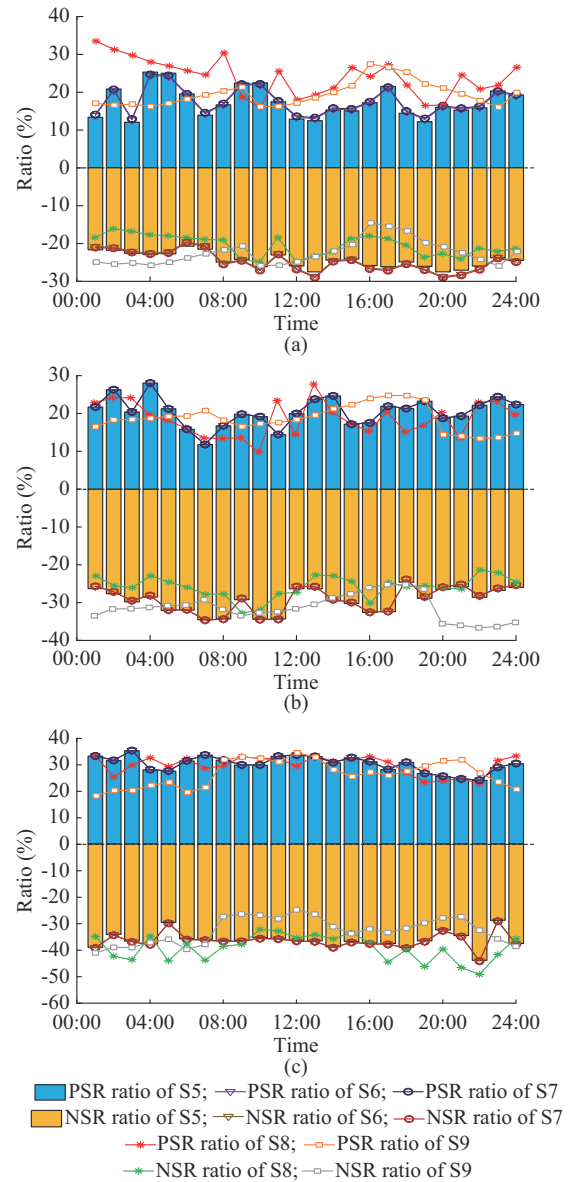


Fig. 9. PSR and NSR ratios of S5-S9. (a) Area 1. (b) Area 2. (c) Area 3.

The results for S8 and S9 indicate that the PSAA incurs an increase of 0.86% in operating cost compared with the MSRO. However, the computation time is reduced by 87%. Therefore, we can conclude that the PSAA provides greater benefits in terms of computation time compared with the MSRO.

By comparing S3 and S5, when the number of units is increased from 33 to 120 while keeping the number of MC samples at 400, the solution time of SAA increases significantly. A comparison of S4 and S8 shows that the computation time of PSAA increases slightly, indicating that PSAA is effective in dealing with large-scale power systems and has a high solution speed.

A comparison of the results presented in Fig. 4 and Table III indicates that when the sample size increases from 200 to 400, the confidence level obtained by SAA increases by approximately 2%, and the corresponding computation cost increases by approximately 6%.

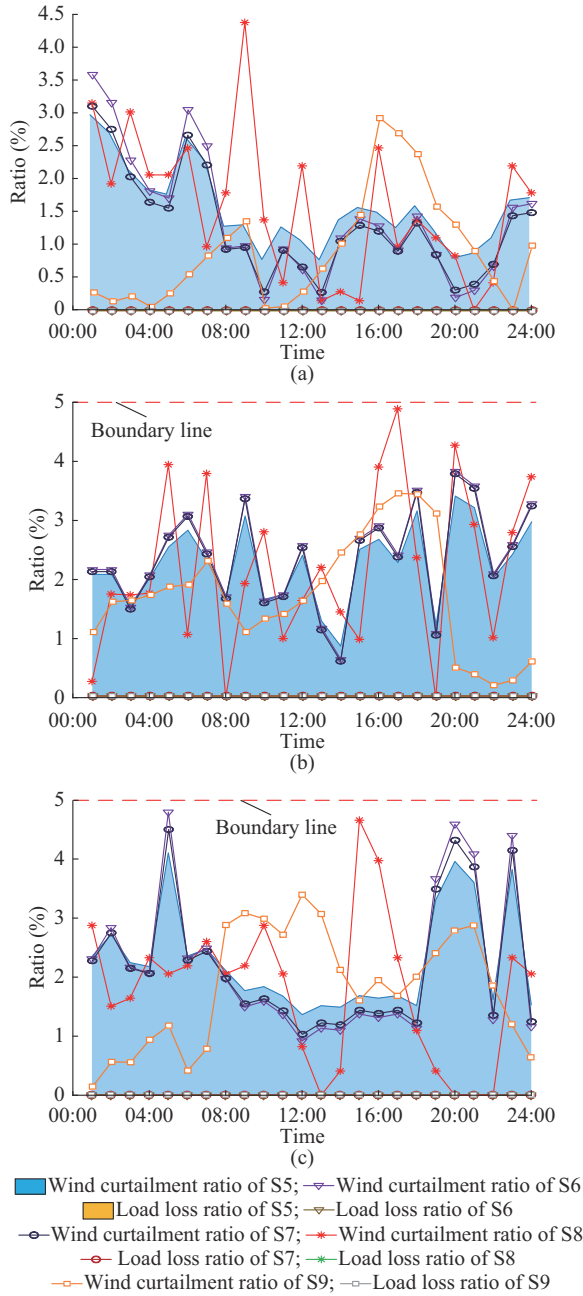


Fig. 10. Wind curtailment and load loss ratios of S5-S9. (a) Area 1. (b) Area 2. (c) Area 3.

TABLE III  
OPERATING COSTS AND COMPUTATION TIME

Case	Scheme	Method	Operating cost (\$)	Computation time (s)
I	S1	SAA	2632149	672.56
	S2	PSAA	2650114	57.33
	S3	SAA	2648824	1793.79
	S4	PSAA	2650838	132.01
II	S5	SAA	4872354	3824.73
	S6	Big- <i>M</i> -SAA	4870457	2417.22
	S7	LHS-SAA	4869175	3621.57
	S8	PSAA	4881442	204.65
	S9	MSRO	4839341	1574.34

However, the confidence level of PSAA remains relatively constant, and its computation time remains stable. In addition, when the number of MC samples is 400, the confidence level of PSAA is higher, resulting in a slightly longer computation time for PSAA compared with that for SAA.

## VII. CONCLUSION

In this paper, a UC problem with JCCs in MAS-WP is investigated. To address the problems of complex analytical computation processes and low computation efficiency of traditional methods, an improved simulation method called PSAA is adopted. The deterministic constraints obtained using PSAA include only continuous variables. Simulation results show that, compared with SAA and other improved methods such as big-*M*-SAA, the PSAA exhibits higher accuracy and efficiency in solving the UC problem with JCCs in MAS-WP.

Future work will consider uncertainties from both the generation and load sides simultaneously in UC problems and extend the PSAA to solve chance-constrained problems involving multiple types of stochastic variables.

## REFERENCES

- [1] S. Xu, W. Wu, B. Wang *et al.*, "Probabilistic energy and reserve co-dispatch for high-renewable power systems and its convex reformulation," *Journal of Modern Power Systems and Clean Energy*, vol. 11, no. 6, pp. 1734-1745, Nov. 2023.
- [2] L. Yang, N. Zhou, G. Zhou *et al.*, "Day-ahead optimal dispatch model for coupled system considering ladder-type ramping rate and flexible spinning reserve of thermal power units," *Journal of Modern Power Systems and Clean Energy*, vol. 10, no. 6, pp. 1482-1493, Nov. 2022.
- [3] Y. Wang, S. Zhao, Z. Zhou *et al.*, "Risk adjustable day-ahead unit commitment with wind power based on chance constrained goal programming," *IEEE Transactions on Power Systems*, vol. 8, no. 2, pp. 530-541, Apr. 2017.
- [4] X. Cao, J. Wang, and B. Zeng, "Networked microgrids planning through chance constrained stochastic conic programming," *IEEE Transactions on Smart Grid*, vol. 10, no. 6, pp. 6619-6628, Nov. 2019.
- [5] Y. Yang, W. Wu, B. Wang *et al.*, "Analytical reformulation for stochastic unit commitment considering wind power uncertainty with Gaussian mixture model," *IEEE Transactions on Power Systems*, vol. 35, no. 4, pp. 2769-2782, Jul. 2020.
- [6] W. Li, Y. Liu, H. Liang *et al.*, "Distributed tracking-ADMM approach for chance-constrained energy management with stochastic wind power in smart grid," *CSEE Journal of Power and Energy Systems*, doi: 10.17775/CSEEJPES.2021.00540
- [7] C. S. Saunders, "Point estimate method addressing correlated wind power for probabilistic optimal power flow," *IEEE Transactions on Power Systems*, vol. 29, no. 3, pp. 1045-1054, May 2014.
- [8] J. Li, J. Wen, S. Cheng *et al.*, "Minimum energy storage for power systems with high wind power penetration using *p*-efficient point theory," *Science China - Information Sciences*, vol. 57, no. 12, pp. 243-254, Dec. 2014.
- [9] S. Cheng, C. Gu, X. Yang *et al.*, "Network pricing for multienergy systems under long-term load growth uncertainty," *IEEE Transactions on Smart Grid*, vol. 13, no. 4, pp. 2715-2729, Jul. 2022.
- [10] C. Duan, W. Fang, L. Jiang *et al.*, "Distributionally robust chance-constrained approximate AC-OPF with Wasserstein metric," *IEEE Transactions on Power Systems*, vol. 33, no. 5, pp. 4924-4936, Sept. 2018.
- [11] A. Prékopa, "Sharp bounds on probabilities using linear programming," *Operations Research*, vol. 38, no. 2, pp. 227-239, Mar. 1990.
- [12] J. Li, L. Lin, Y. Xu *et al.*, "Probability efficient point method to solve joint chance-constrained unit commitment for multi-area power systems with renewable energy," *IEEE Transactions on Power Systems*, vol. 38, no. 3, pp. 2120-2133, May 2023.
- [13] Y. Huang, L. Wang, W. Guo *et al.*, "Chance constrained optimization in a home energy management system," *IEEE Transactions on Smart Grid*, vol. 9, no. 1, pp. 252-260, Jan. 2018.

- [14] C. S. Saunders, "Point estimate method addressing correlated wind power for probabilistic optimal power flow," *IEEE Transactions on Power Systems*, vol. 29, no. 3, pp. 1045-1054, May 2014.
- [15] U. A. Ozturk, M. Mazumdar, and B. A. Norman, "A solution to the stochastic unit commitment problem using chance constrained programming," *IEEE Transactions on Power Systems*, vol. 19, no. 3, pp. 1589-1598, Aug. 2004.
- [16] J. Huang, Y. Xue, Z. Y. Dong *et al.*, "An adaptive importance sampling method for probabilistic optimal power flow," in *Proceedings of 2011 IEEE PES General Meeting*, Detroit, USA, Jul. 2011, pp. 1-6.
- [17] B. Zou and Q. Xiao, "Solving probabilistic optimal power flow problem using quasi Monte Carlo method and ninth-order polynomial normal transformation," *IEEE Transactions on Power Systems*, vol. 29, no. 1, pp. 300-306, Jan. 2014.
- [18] B. Basciftci, S. Ahmed, N. Z. Gebraeel *et al.*, "Stochastic optimization of maintenance and operations schedules under unexpected failures," *IEEE Transactions on Power Systems*, vol. 33, no. 6, pp. 6755-6765, Nov. 2018.
- [19] E. D. Anese, K. Baker, and T. Summers, "Chance-constrained AC optimal power flow for distribution systems with renewables," *IEEE Transactions on Power Systems*, vol. 32, no. 5, pp. 3427-3438, Sept. 2017.
- [20] Z. Wu, P. Zeng, X. P. Zhang *et al.*, "A solution to the chance-constrained two-stage stochastic program for unit commitment with wind energy integration," *IEEE Transactions on Power Systems*, vol. 31, no. 6, pp. 4185-4196, Nov. 2016.
- [21] G. Wu, Y. Xiang, J. Liu *et al.*, "Chance-constrained optimal dispatch of integrated electricity and natural gas systems considering medium and long-term electricity transactions," *CSEE Journal of Power and Energy Systems*, vol. 5, no. 3, pp. 315-323, Sept. 2019.
- [22] S. Lu, H. Su, C. Johnsson *et al.*, "A chance constrained programming approach for multi-product multi-stage integrated production planning under internal and external uncertainties," in *Proceedings of 2015 IEEE International Conference on Automation Science and Engineering (CASE)*, Gothenburg, Sweden, Aug. 2015, pp. 880-885.
- [23] Y. Zhang, J. Wang, B. Zeng *et al.*, "Chance-constrained two-stage unit commitment under uncertain load and wind power output using bilinear benders decomposition," *IEEE Transactions on Power Systems*, vol. 32, no. 5, pp. 3637-3647, Sept. 2017.
- [24] F. Qiu and J. Wang, "Chance-constrained transmission switching with guaranteed wind power utilization," *IEEE Transactions on Power Systems*, vol. 30, no. 3, pp. 1270-1278, May 2015.
- [25] Y. Song, J. R. Luedtke, and S. Küçükyavuz, "Chance-constrained binary packing problems," *INFORMS Journal on Computing*, vol. 26, no. 4, pp. 735-747, May 2015.
- [26] K. Seddig, P. Jochem, and W. Fichtner, "Two-stage stochastic optimization for cost-minimal charging of electric vehicles at public charging stations with photovoltaics," *Applied Energy*, vol. 242, pp. 769-781, Mar. 2019.
- [27] K. Simge, "On mixing sets arising in chance-constrained programming," *Mathematical Programming*, vol. 132, no. 1-2, pp. 31-56, May 2010.
- [28] B. Zeng, Y. An, and K. Ludwig, "Chance constrained mixed integer program: bilinear and linear formulations, and benders decomposition," Tech. Rep., University of South Florida, Tampa, USA, 2014.
- [29] B. K. Pagnoncelli, S. Ahmed, and A. Shapiro, "Sample average approximation method for chance constrained programming: theory and applications," *Journal Optimization Theory Applications*, vol. 142 no. 2, pp. 399-416, Mar. 2009.
- [30] S. Jiang, J. Cheng, K. Pan *et al.*, "Data-driven chance-constrained planning for distributed generation: a partial sampling approach," *IEEE Transactions on Power Systems*, vol. 38, no. 6, pp. 5228-5244, Nov. 2023.
- [31] Z. Liu, S. Liu, Q. Li *et al.*, "Optimal day-ahead scheduling of islanded microgrid considering risk-based reserve decision," *Journal of Modern Power Systems and Clean Energy*, vol. 9, no. 5, pp. 1149-1160, Sept. 2021.
- [32] C. Lowery and M. O'Malley, "Reserves in stochastic unit commitment: An Irish system case study," *IEEE Transactions on Sustainable Energy*, vol. 6, no. 3, pp. 1029-1038, Jul. 2015.
- [33] J. Wang, H. Zhong, Z. Yang *et al.*, "Incentive mechanism for clearing energy and reserve markets in multi-area power systems," *IEEE Transactions on Sustainable Energy*, vol. 11, no. 4, pp. 2470-2482, Oct. 2020.
- [34] J. Xu, S. Liao, H. Jiang *et al.*, "A multi-time scale tie-line energy and reserve allocation model considering wind power uncertainties for multi-systems," *CSEE Journal of Power and Energy Systems*, vol. 7, no. 4, pp. 677-687, Jul. 2021.
- [35] R. Karimi, J. Cheng and M. A. Lejeune, "A framework for solving chance-constrained linear matrix inequality programs," *INFORMS Journal on Computing*, vol. 33, no 3, pp. 1015-1036, Feb. 2021.
- [36] GI. Nagy, G. Barta, S. Kazi *et al.*, "GEFCom2014: probabilistic solar and wind power forecasting using a generalized additive tree ensemble approach," *International Journal of Forecasting*, vol. 32, no. 3, pp. 1087-1093, Jul. 2016.
- [37] H. Xiong, Y. Shi, Z. Chen *et al.*, "Multi-stage robust dynamic unit commitment based on pre-extended-fast robust dual dynamic programming," *IEEE Transactions on Power Systems*, vol. 38, no. 3, pp. 2411-2422, May 2023.

**Jinghua Li** received the B.S. and M.S. degrees in power engineering from North China Electric Power University, Beijing, China, and the Ph.D. degree in power engineering from Guangxi University, Nanning, China, in 2011. She was a Postdoctoral Researcher in electrical engineering, Huazhong University of Science and Technology, Wuhan, China, from 2012 to 2014. Now she is a Professor and Ph.D. supervisor of the Department of Electrical Engineering, Guangxi University, Nanning, China. Her main research interests include power system operation and planning, particularly in application of optimization methods to power systems.

**Hongyu Zeng** received the B.S. degree in electrical engineering from Southwest University, Chongqing, China, in 2021. He is currently pursuing the M.S. degree at Guangxi University, Nanning, China. His main research interests include power system operation and planning.

**Yutian Xie** received the B.S. degree in electrical engineering from Northeast Electric Power University, Jilin, China, in 2020. He is currently pursuing the M.S. degree at Guangxi University, Nanning, China. His main research interests include power system operation and planning.